*Int. J. Solids Structures* Vol. 23, No. 3, pp. 387–402, 1987
Printed in Great Britain.

0020-7683/87 $3.00+.00


# THERMAL VISCOPLASTIC BUCKLING DURING THE GROWTH OF SILICON RIBBON

C. T. TSAI and O. W. DILLON, JR.
Department of Engineering Mechanics, University of Kentucky, Lexington, KY 40506, U.S.A.

(*Received* 28 *February* 1986; *in revised form* 18 *June* 1986)

**Abstract**—This paper is an analysis of the conditions to be satisfied in order to avoid buckling during the growth of a silicon ribbon that is being slowly pulled from the melt. A viscoplastic constitutive equation with a dislocation density effect is used to model the material behavior. The critical thicknesses and the corresponding deflection shapes are calculated by the finite element method for the cantilever boundary conditions. The value of the parameter which controls the speed of the lateral deflection is computed by using Galerkin's method. It is demonstrated that, due to the effect of viscoplasticity, some deflection shapes increase in magnitude with time and other shapes damp out.

## 1. INTRODUCTION

One approach to lowering the cost of solar power involves producing thin sheets of high quality silicon ribbon (very thin plate) directly from the molten state. These sheets are subsequently processed into photovoltaic cells. In order to make the economics of silicon favorable for photovoltaics, it is necessary to have high productivity of the ribbon material. This implies that wide sheets must be produced under conditions which require rapid cooling at the solid–liquid interface. These conditions produce very non-uniform thermal fields which generate large thermal stresses. These large thermal stresses can cause buckling of the wide thin silicon ribbon[1–4].

In silicon ribbon growing processes, buckling phenomena are the most severe limitation to the growth of good quality wider ribbon. Both the magnitude of the thermal stresses and the stiffness of the ribbon depend on the value of the width. Simply said, processes which produce good ribbon that is 2 cm in width do not yield the same quality product that is 10 cm wide. Industrial experience is that the type of buckling that develops depends on the details of the process used to grow the ribbon. Some processes have buckles which are of long wavelengths[4] while others have very short wavelength[2] permanent deformations. Duncan *et al.*[1], Kalejs *et al.*[2], Gurtler[5] and Dillon and De Angelis[6] have contributed to the elastic buckling analysis of this problem. However it is clear that the stresses in part of the ribbon are far above the local yield stress and this raises questions about the applicability of the elastic analysis.

Basic work on the material response functions for silicon was done by Haasen[7, 8] and Sumino and co-workers[9, 10]. They found that silicon is a viscoplastic material at constant temperature and has an $\exp(-Q/kT')$ type correlation between its responses at different temperatures. They also found that the response depended on the dislocation density. The efficiency of solar cells as power generators is also related to their dislocation density[11, 12]. It is ideal when the maximum dislocation density can be kept below $10^4$ $cm^{-2}$[1, 3]. This is, of course, a very different parameter domain than the $10^9\,cm^{-2}$ which usually exists in metals. This low dislocation density forces us to simultaneously make calculations on the dislocation density spatial distributions just as we predict the stress distributions[13].

This analysis parallels that of Tvergaard[14], in several important details, who considered the creep buckling of simply supported plates subjected to constant axial stresses in one direction. Our analysis differs from that of Tvergaard in the material constitutive relation that is used and the nature of the stresses involved. The in-plane stresses considered herein are due to the non-uniform thermal profile and therefore all components (i.e. $\sigma^0_{yy}$, $\sigma^0_{yy}$ and $\sigma^0_{yy}$) exist, vary in space and must be retained[15, 16]. The

ribbon is considered to be very thin and the strain is assumed linear through the thickness and there is no coupling between the in-plane forces and bending so that the in-plane forces do not change during buckling. A finite element method is used to calculate the critical thicknesses and the corresponding buckling shapes, and Galerkin's method is used to determine how the amplitudes of the lateral deflection grow in time[13].

## 2. ANALYSIS

Consider a plate having a small initial imperfection $w^0$, the governing differential equation is[15–17]

$$\frac{\partial^2 M_x}{\partial x^2} + 2\frac{\partial^2 M_{xy}}{\partial x \partial y} + \frac{\partial^2 M_y}{\partial t^2} = -P_z(x,y) - h\sigma^0_{xx}\frac{\partial^2 w}{\partial x^2} - 2h\sigma^0_{xy}\frac{\partial^2 w}{\partial x \partial y} - h\sigma^0_{yy}\frac{\partial^2 w}{\partial y^2}. \tag{1}$$

The rectangular Cartesian coordinate system $(x, y)$ that is used is shown in Fig. 1. The in-plane stresses from the prebuckling state are denoted $\sigma^0_{yy}$, $\sigma^0_{yy}$ and $\sigma^0_{yy}$ and $h$ is the plate thickness; $M_x$, $M_{xy}$ and $M_y$ are the moments in the buckling state. The total lateral deflection of the plate is $w$ and $P_z(x, y)$ is the lateral load intensity that is applied to the plate.

The material response is assumed to be isotropic and thermal viscoplastic such that[13]

$$\dot{\varepsilon}_{ij} = \frac{1+\nu}{E}\dot{\sigma}_{ij} - \frac{\nu}{E}\dot{\sigma}_{kk}\delta_{ij} + \alpha\dot{T}\delta_{ij} + \dot{\varepsilon}^{\mathrm{pl}}_{ij}(\sigma_{ij}, N_{\mathrm{m}}) \tag{2}$$

where $i, j, k = 1, 2, 3$, $\dot{\sigma}_{ij}$ are the components of the stress rate tensor, $\dot{\varepsilon}_{ij}$ are the components of the strain rate tensor, $\dot{T}$ is the rate of change of temperature, $\dot{\varepsilon}^{\mathrm{pl}}_{ij}$ are components of the plastic strain rate tensor, $N_{\mathrm{m}}$ is the mobile dislocation density, $\delta_{ij}$ is the Kronecker delta function, $\alpha$ is the thermal expansion coefficient, $\nu$ is Poisson's ratio, and $E$ is Young's modulus which is a function of temperature and is given as $1.7 \times 10^{11} - 2.771 \times 10^4 \times (T')^2$ Pa, where $T'$ is the absolute temperature[18]. The plastic strain rates in eqn (2) are written as[13, 14]

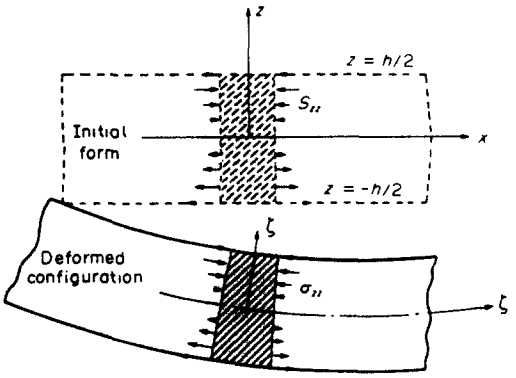


Fig. 1. The typical plate element in its initial and deformed configuration.

$$\dot{\varepsilon}_{ij}^{pl} = fS_{ij} \tag{3}$$

and the rate of dislocation density change is[13]

$$\dot{N}_m = KN_m k_0 e^{-Q/kT'}(\sqrt{J_2} - D\sqrt{N_m})^{p+r} \tag{4}$$

where $S_{ij}$ are deviatoric components of the stress tensor defined by $S_{ij} = \sigma_{ij} - \sigma_{kk}\delta_{ij}/3$. The viscosity $f$ in eqn (3) is[13]

$$f = N_m k_0 b e^{-Q/kT'}(\sqrt{J_2} - D\sqrt{N_m})^p \frac{1}{\sqrt{J_2}} \tag{5}$$

if $\sqrt{J_2} \leqslant D\sqrt{N_m}$, the values of $f$ and $\dot{N}_m$ are zero, and where

$$k_0 = B_0/\tau_0^p, \qquad D = Gb/B, \qquad (\cdot) \equiv \frac{\partial(\,)}{\partial t}$$

$t$ is time and $\tau$ is the "applied shear stress"; $G$ is the shear modulus; $b$ is the magnitude of Burger's vector which for silicon is $3.8 \times 10^{-10}$ m; $N_m$ is the density of mobile dislocation; $B$ is a parameter characterizing the interaction between dislocations and is 3.3; $Q$ is the Peierls energy and is 2.17 eV; $k$ is Boltzman's constant and is equal to $8.617 \times 10^{-5}$ eV K$^{-1}$; $B_0$ is mobility and is taken as $4.3 \times 10^4$ m$^{-1}$; $K$, $p$ and $r$ are material constants which are taken as $3.1 \times 10^{-4}$ m N$^{-1}$, 1.1 and 1.0, respectively; and $\tau_0$ is assumed to be equal to $10^7$ N m$^{-2}$. The parameter $J_2 = (S_{ij}S_{ij})/2$ is the second invariant of the deviatoric stress tensor and $D\sqrt{N_m}$ is called the back stress. The form of eqns (4) and (5), as well as the numerical values for the constants therein are based on the work of Haasen[7, 8] and Sumino and co-workers[9, 10] in the one-dimensional test. Silicon is also anisotropic in its elastic response. We assume isotropy in order to evaluate the effect of the viscoplastic response on buckling.

We now find it convenient to write the total lateral deflection $w$ as

$$w = w^e + w^{vp} + w^0 \tag{6}$$

where superscripts e and vp represent elastic and plastic behavior, respectively, and $w^0$ is the initial lateral imperfection. The strains are also split into in-plane components plus bending terms and written as

$$\varepsilon_{ij} = \varepsilon_{ij}^0 - z\frac{\partial^2(w^e + w^{vp})}{\partial x_i \partial x_j} \tag{7a}$$

where $\varepsilon_{ij}^0$ is the strain in the middle plane of the plate and $z$ is the distance from the middle plane. By making the time derivative of eqn (7a), we have

$$\dot{\varepsilon}_{ij} = \dot{\varepsilon}_{ij}^0 - z\frac{\partial^2(\dot{w}^e + \dot{w}^{vp})}{\partial x_i \partial x_j} \tag{7b}$$

where the dot on the top of each variable is the rate of its variable. The basic definition

$$M_{ij} = \int_{-h/2}^{h/2} \sigma_{ij} z \, dz \tag{8}$$

relates the stresses $\sigma_{ij}$ to the moments.

When elastic strains are considered separately (i.e. plastic strain rates are zero), the

moment tensor can be expressed in terms of the elastic lateral deflection $w^e$ alone according to eqn (7a). They are

$$M_x = -D_e\left(\frac{\partial^2 w^e}{\partial x^2} + \nu\frac{\partial^2 w^e}{\partial y^2}\right)$$

$$M_y = -D_e\left(\frac{\partial^2 w^e}{\partial y^2} + \nu\frac{\partial^2 w^e}{\partial x^2}\right) \tag{9}$$

$$M_{xy} = -D_e(1-\nu)\frac{\partial^2 w^e}{\partial x \partial y}$$

where

$$D_e = \frac{Eh^3}{12(1-\nu^2)}.$$

When the elastic strain rates are zero, the moments acting on the plates are expressed in terms of the viscoplastic lateral deflection rate $\dot{w}^{vp}$ alone according to eqn (7b). They are

$$M_x = -D_{vp}\left(2\frac{\partial^2 \dot{w}^{vp}}{\partial x^2} + \frac{\partial^2 \dot{w}^{vp}}{\partial y^2}\right)$$

$$M_y = -D_{vp}\left(2\frac{\partial^2 \dot{w}^{vp}}{\partial y^2} + \frac{\partial^2 \dot{w}^{vp}}{\partial x^2}\right) \tag{10}$$

and

$$M_{xy} = -D_{vp}\frac{\partial^2 \dot{w}^{vp}}{\partial x \partial y}$$

where

$$D_{vp} = \frac{h^3}{12f}$$

where the viscosity $f$, as defined in eqn (5), is a complex function of $x$ and $y$ but is "known" in the buckling analysis[13, 19], and in particular is assumed to be independent of the thickness position. One can interpret $f$ being independent of $z$ to be a Taylor series expansion where the first term is all that is retained.

Since the definition of eqn (8) is true regardless of the material properties, under the same applied loading circumstances, the relationship between the elastic lateral deflection $w^e$ and the viscoplastic lateral deflection rate $\dot{w}^{vp}$ can be written as

$$\frac{\partial^2 \dot{w}^{vp}}{\partial x^2} = EVP\left(\frac{\partial^2 w^e}{\partial x^2}(2-\nu) + (2\nu-1)\frac{\partial^2 w^e}{\partial y^2}\right)$$

$$\frac{\partial^2 \dot{w}^{vp}}{\partial y^2} = EVP\left(\frac{\partial^2 w^e}{\partial y^2}(2-\nu) + (2\nu-1)\frac{\partial^2 w^e}{\partial x^2}\right) \tag{11}$$

$$\frac{\partial^2 \dot{w}^{vp}}{\partial x \partial y} = 3EVP(1-\nu)\frac{\partial^2 w^e}{\partial x \partial y}$$

where

$$EVP = \frac{fE}{3(1-\nu^2)}.$$

For small plastic deformations, there is no volume change and Poisson's ratio $\nu$ is assumed as 0.5 in the elastic range as well. Hence eqn (11) becomes

$$\frac{\partial^2 \dot{w}^{vp}}{\partial x^2} = \frac{2fE}{3}\frac{\partial^2 w^e}{\partial x^2}$$
$$\frac{\partial^2 \dot{w}^{vp}}{\partial y^2} = \frac{2fE}{3}\frac{\partial^2 w^e}{\partial y^2} \tag{12}$$
$$\frac{\partial^2 \dot{w}^{vp}}{\partial x \partial y} = \frac{2fE}{3}\frac{\partial^2 w^e}{\partial x \partial y}.$$

This is one of the key ideas in Tvergaard's analysis. We then use eqn (1), where the lateral load intensity $P_z(x, y)$ is assumed zero during the growth of the ribbon, and eqn (7) to produce

$$\frac{D_e}{h}\nabla^4 w^e = \sigma_{xx}^0 \frac{\partial^2 (w^e + w^{vp} + w^0)}{\partial x^2} + 2\sigma_{xy}^0 \frac{\partial^2 (w^e + w^{vp} + w^0)}{\partial x \partial y} + \sigma_{yy}^0 \frac{\partial^2 (w^e + w^{vp} + w^0)}{\partial y^2}. \tag{13}$$

Since we assume that the in-plane forces do not change during buckling, the time derivative of the in-plane stresses vanishes. The initial imperfection $w^0$ is a known deflected shape and does not change with time, so that its time derivative also vanishes. By taking the time derivative of both sides of eqn (13), we obtain

$$\frac{D_e}{h}\nabla^4 \dot{w}^e = \sigma_{xx}^0 \frac{\partial^2 (\dot{w}^e + \dot{w}^{vp})}{\partial x^2} + 2\sigma_{xy}^0 \frac{\partial^2 (\dot{w} + \dot{w}^{vp})}{\partial x \partial y} + \sigma_{yy}^0 \frac{\partial^2 (\dot{w}_e + \dot{w}^{vp})}{\partial y^2}. \tag{14}$$

This eliminates $w^0$ from eqn (13). By substituting eqn (12) into eqn (14), we obtain

$$\frac{D_e}{h}\nabla^4 \dot{w}^e = \sigma_{xx}^0 \frac{\partial^2 \dot{w}^e}{\partial x^2} + 2\sigma_{xy}^0 \frac{\partial^2 \dot{w}^e}{\partial x \partial y} + \sigma_{yy}^0 \frac{\partial^2 \dot{w}^e}{\partial y^2} + \frac{2fE}{3}\left(\sigma_{xx}^0 \frac{\partial^2 w^e}{\partial x^2} + 2\sigma_{xy}^0 \frac{\partial^2 w^e}{\partial x \partial y} + \sigma_{yy}^0 \frac{\partial^2 w^e}{\partial y^2}\right). \tag{15}$$

Equation (15) is the governing equation of buckling for a viscoplastic plate, but due to eqn (12), it involves only the elastic deflection $w^e$ as the dependent variable. This does not mean that the plate is being considered as an elastic one. Equation (15) is a typical creep buckling type equation for plates whose solution can be assumed in the separable form as

$$w^e(x, y, t) = g(t)W(x, y) \tag{16}$$

where $W(x, y)$ is the deflected shape of the plates and $g(t)$ is the magnitude of the deflected shape.

2.1. *Analysis with the prescribed deflection shape (simply supported plate)*

If the deflected shape of the plates is approximately known before the buckling analysis begins, the solution procedures are similar to those of Tvergaard[14] as illustrated in the appendix for our material.

2.2. *Analysis without the prescribed deflection shape*

If the approximate buckling mode shape for creep buckling is not available beforehand, the Tvergaard solution technique must be somewhat modified. By substituting eqn (16) into eqn (15), we obtain

$$\frac{\dot{g}(t)}{g(t)} = \frac{\dfrac{2fE}{3}\left(\sigma^0_{xx}\dfrac{\partial^2 W}{\partial x^2} + 2\sigma^0_{xy}\dfrac{\partial^2 W}{\partial x \partial y} + \sigma^0_{yy}\dfrac{\partial^2 W}{\partial y^2}\right)}{\dfrac{D_e}{h}\nabla^4 W - \sigma^0_{xx}\dfrac{\partial^2 W}{\partial x^2} - 2\sigma^0_{xy}\dfrac{\partial^2 W}{\partial x \partial y} - \sigma^0_{yy}\dfrac{\partial^2 W}{\partial y^2}} = \lambda^2 \tag{17}$$

where $\lambda^2$ is the separation parameter. From eqn (17), two differential equations are obtained. One is for the time-dependent amplitude problem and the other is the spatial problem. They are

$$\dot{g}(t) - \lambda^2 g(t) = 0 \tag{18}$$

and

$$D_e\nabla^4 W - \left(1 + \frac{2fE}{3\lambda^2}\right)h\left(\sigma^0_{xx}\frac{\partial^2 W}{\partial x^2} + 2\sigma^0_{xy}\frac{\partial^2 W}{\partial x \partial y} + \sigma^0_{yy}\frac{\partial^2 W}{\partial y^2}\right) = 0. \tag{19}$$

When the value of $f$ vanishes, eqn (19) becomes the governing equation of elastic plate buckling. Hence, the viscoplastic buckling shape is governed by the same spatial equation as the elastic buckling one but where the elastic in-plane forces have to be replaced by

$$\left(1 + \frac{2fE}{3\lambda^2}\right)h\sigma_{ij}. \tag{20}$$

Of course the plate made of inelastic material also has deflections which grow with time according to eqn (18). The solution of eqn (18) is

$$g(t) = g^0 e^{\lambda^2 t} \tag{21}$$

where $g^0$ is the amplitude of the initial plate imperfection $w^0$ whose deflection shape is $W(x, y)$. The value of $\lambda^2$ controls the speed of the lateral deflection of plates. When the value of $\lambda^2$ is equal to infinity, elastic buckling occurs at once. A large value of $\lambda^2$ means that the lateral deflection of plates grow rapidly. When $\lambda^2$ is negative, the initial imperfection of plates will damp out with time.

If one assumes that $fE/\lambda^2 \ll 1$, eqn (19) reduces to

$$\frac{D_e}{h}\nabla^4 W = \sigma^0_{xx}\frac{\partial^2 W}{\partial x^2} + 2\sigma^0_{xy}\frac{\partial^2 W}{\partial x \partial y} + \sigma^0_{yy}\frac{\partial^2 W}{\partial y^2}. \tag{22}$$

Equation (22) is the case of elastic plate buckling, except that the in-plane stresses are the viscoplastic ones and therefore this equation can be solved by standard finite element methods[13, 20–23] in order to calculate the critical thicknesses (i.e. $\sqrt{(1/\text{eigenvalue})}$) and the corresponding mode shapes. In all thermal buckling problems discussed herein, the in-plane stresses $\sigma^0_{ij}$ are calculated from the prebuckling state[13, 19], where the material is considered to be viscoplastic and governed by eqns (2)–(5).

Let the critical thicknesses found from eqn (22) be designated as $h_{cr}$ and the corresponding buckling mode shapes be $W^*(x, y)$, then eqn (22) becomes

$$\frac{D^{cr}_e}{h_{cr}}\nabla^4 W^* = \sigma^0_{xx}\frac{\partial^2 W^*}{\partial x^2} + 2\sigma^0_{xy}\frac{\partial^2 W^*}{\partial x \partial y} + \sigma^0_{yy}\frac{\partial^2 W^*}{\partial y^2}. \tag{23}$$

By substituting eqn (23) into eqn (19), we obtain

$$\frac{D_e}{h}\nabla^4 W^* - \left(1 + \frac{2fE}{3\lambda^2}\right)\frac{D^{cr}_e}{h_{cr}}\nabla^4 W^* = 0. \tag{24}$$

Since the values of $f$ and $E$ vary throughout the plane of the plate, Galerkin's method

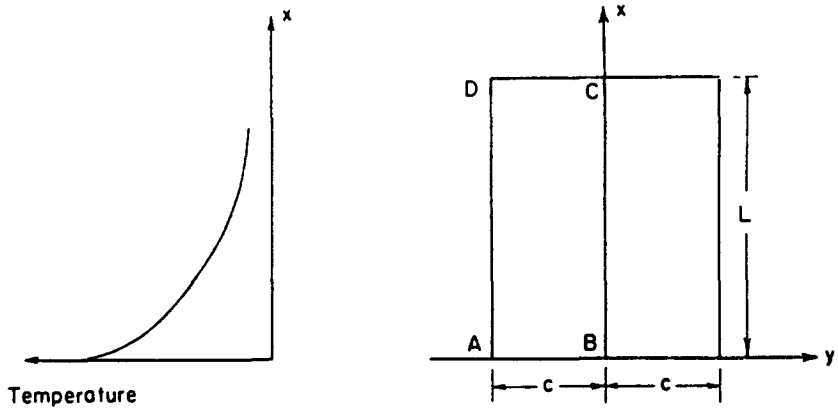


Fig. 2. Dimensions of the ribbon and the schematic thermal profile along the growth (x) direction.

can be used to evaluate the value of $\lambda^2$ for the entire plate deflecting as a unit[13]. By multiplying eqn (24) by $W^*(x, y)$ and integrating the result throughout the plane of the plate, we obtain

$$\lambda^2 = \frac{h_{cr}^2}{h^2 - h_{cr}^2} \frac{S1}{S2} \tag{25}$$

where

$$S1 = \int_0^a \int_0^b \frac{2fE}{3} (\nabla^4 W^*) W^* \, dx \, dy, \qquad S2 = \int_0^a \int_0^b E(\nabla^4 W^*) W^* \, dx \, dy$$

and $h$ is the actual plate thickness (which is larger than $h_{cr}$).

In formulating the above problem we linearize the plastic strain variation in the $z$-direction; $f$ is calculated from the stresses and dislocation densities in the $z = 0$ plane and is assumed independent of $z$. The result is eqn (21). Had the $z$ dependence in $f$ been retained, the analogue of eqn (21) would predict infinite deflections in a finite time. However, our interest is in avoiding large deflections and therefore the assumption of $f$ being independent of $z$ is adequate and much simpler to use. In order to evaluate the integrals in eqn (25), we use $W^*(x, y)$ as given by the FEM solution of eqn (23) as the approximate deflection shape in the Galerkin procedure.

## 3. NUMERICAL RESULTS FOR CANTILEVER SILICON RIBBON

In growing silicon ribbon, a fixed boundary is assumed in bending along the far end ($x = L$) of the ribbon and the other boundaries are all traction free as shown in Fig. 2. Therefore, a creep buckling analysis of the cantilever rectangular plates will be used as the model of growing ribbon. A finite element program was developed for the IBM 3083 computer. A 16 degrees of freedom Hermitian-conforming rectangular element is used. There are four nodes in each element and four degrees of freedom (i.e. $w$, $\partial w/\partial x$, $\partial w/\partial y$ and $\partial^2 w/\partial x \partial y$) at each node[13, 20, 21]. Therefore, the values of $w$, $\partial w/\partial x$, $\partial w/\partial y$ and $\partial w^2/\partial x \partial y$ are zero along the fixed edge and arbitrary along the free edge[13].

A simply supported elastic plate which is subjected to an axial compression force in one direction was used to test the accuracy of the program. When a quarter plate (because of symmetry) is divided into four elements, the difference between the exact and finite element values of the critical load is 0.6% when using single precision numerics in the computer. When the elastic quarter plate is divided into 16 elements, the difference in the

buckling load is about 0.1%[13]. If more elements (say more than 50 elements) are used, double precision arithmetic is required in the computer in order to reduce roundoff errors. The plate is divided into 20 × 20 elements in this paper. This results in a large system of linear algebraic equations where many of the low eigenvalues (critical thicknesses) and the corresponding eigenvectors (buckling mode shapes) for eqn (22) are calculated by the computer. Since some eigenvalues are negative, the number of eigenvalues which are specified to be solved for in the computer calculation must be larger than the number of negative eigenvalues in eqn (22)[13]. We frequently find it necessary to calculate 30 eigenvalues. After the critical thicknesses and the corresponding mode shapes $W(x, y)$ are obtained, the actual plate thickness $h$, which is taken to be larger than the critical thickness $h_{cr}$ of the first positive buckling mode (the lowest positive eigenvalue), is chosen. By substituting these values into eqn (25), the values of $\lambda^2$ are computed. The negative eigenvalues means that the plate will buckle when the in-plane stresses have the same spatial distribution but have a change in sign. Since this change in sign cannot occur for the prescribed thermal fields, there is no physical content in these values.

The in-plane stresses used here are obtained from the viscoplastic plane stress analysis[13]. The in-plane thermal stresses $\sigma^0_{yy}$, $\sigma^0_{yy}$ and $\sigma^0_{yy}$ in the prebuckling state are calculated before attempting the buckling analysis. The equilibrium equation for the in-plane stresses in a thin plate lying in the $x$–$y$ plane is used in the form[13]

$$\frac{\partial^2 \sigma^0_{xx}}{\partial x^2} - \frac{\partial^2 \sigma^0_{yy}}{\partial y^2} = 0 \tag{26}$$

and the compatibility equation becomes

$$\nabla^2(\sigma^0_{xx} + \sigma^0_{yy} + \alpha ET) = -FP \tag{27}$$

where

$$FP = \frac{1}{V}\int_0^x E\left(\frac{\partial^2 \dot{\varepsilon}^{pl}_{xx0}}{\partial y^2} + \frac{\partial^2 \dot{\varepsilon}^{pl}_{yy0}}{\partial x^2} - 2\frac{\partial^2 \dot{\varepsilon}^{pl}_{xy0}}{\partial x \partial y}\right) dx \tag{28}$$

where $\dot{\varepsilon}^{pl}_{yy0}$, $\dot{\varepsilon}^{pl}_{yy0}$ and $\dot{\varepsilon}^{pl}_{yy0}$ are the plastic strain rates in the prebuckling state, and $V$ is the pull speed of the silicon ribbon and is taken to be 3 cm min$^{-1}$ in this analysis. Equations (26)–(28), plus eqn (5), and the traction-free boundary conditions of the plate are solved iteratively to yield $\sigma^0_{yy}$, $\sigma^0_{yy}$, $\sigma^0_{yy}$ and $N_m$ as functions of space $(x, y)$. It is found that there is a critical width for which the iteration process that is used converges. The stresses in wide ribbons become large which creates a high dislocation density and ultimately the plastic strain rates become too large.

Typical results for $\sigma^0_{yy}(x, y)$ and $N(x, y)$ are shown in Figs 3 and 4. Details of the solutions of eqns (26)–(28) and additional results are contained in recent publications[13, 19].

A quadratic and an exponential thermal profile will be used as examples of thermal fields that can be analyzed. The creep buckling analysis and results will be discussed below for these profiles.

### 3.1. *The quadratic thermal profile*

Consider now the case where the ribbon length is 8 cm, the initial dislocation density is 0.5 cm$^{-2}$ and the pull speed is 3 cm min$^{-1}$. This ribbon is subjected to the quadratic thermal profile given by $T(x) = 1412 - 110.74x + 3.5x^2$°C. The in-plane stresses and the values of viscosity $f$ are obtained by solving eqns (26)–(28)[13, 19]. The specific value of $\lambda^2$ is calculated by assuming (arbitrarily) the actual plate thickness to be $h = 1.1h_{cr}$, where $h_{cr}$ is the thickness of the first positive buckling mode. The critical thickness and the value of $\lambda^2$ for each corresponding buckling mode are shown in Tables 1–3 for plate widths of 8, 6 and 4 cm. Results (critical thicknesses and $\lambda^2$) obtained for an 8 cm wide ribbon are

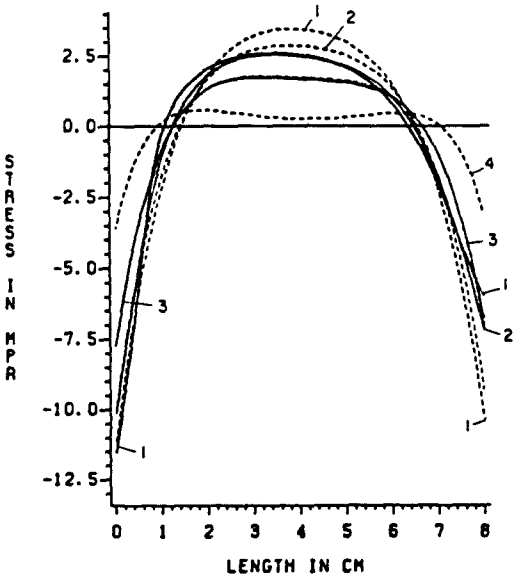


Fig. 3. The elastic and viscoplastic stresses $\sigma_{yy}$ along the ribbon centerline for $T = 1440e^{-0.08x}$ for several plate widths. Solid lines represent stresses in a plastic material while the dashed lines are for an elastic substance. Lines 1, 2 and 3 are for plate widths of 7.5, 7 and 6 cm, respectively. Dashed line 4 is for a 4 cm wide plate where the stresses are the same in an elastic and viscoplastic plate.

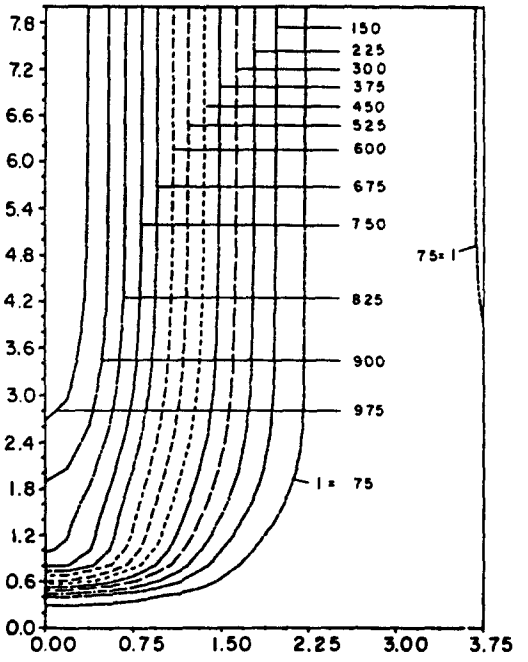


Fig. 4. The dislocation density contour plate for an 8 × 7.5 cm plate having an initial dislocation density of 0.5 $cm^{-2}$. The thermal profile is $T(x) = 1440e^{-0.08x}$.

given in Table 1. Clearly, the second mode shape in Table 1 has the maximum value of $\lambda^2$ (or lateral growing speed). The mode shapes for the first and second buckling modes for a ribbon width of 8 cm are shown in Figs 5 and 6. Results for a 6 cm wide ribbon are give in Table 2. The second mode again has the maximum value of $\lambda^2$. Table 3 contains results for a 4 cm wide ribbon. The buckling mode with the fastest lateral growing speed for the 4 cm wide ribbon is the first one. The first buckling mode for this profile (and these

Table 1. The critical thicknesses and values of $\lambda^2$ for several modes of an 8 × 8 cm plate subjected to a $T(x) = 1412 - 110.74x + 3.5x^2$ (°C). The initial dislocation density is 0.5 $cm^{-2}$ and the actual thickness $h$ used to calculate $\lambda^2$ was 1.1 $h_{cr}$ (0.288 mm) of the first mode. The fastest growing mode is the second one

| Mode | $h_{cr}$(mm) | $\lambda^2(s^{-1})$ |
|---|---|---|
| 1 | 0.262 | 0.0452 |
| 2 | 0.258 | 0.0868 |
| 3 | 0.203 | 0.000175 |
| 4 | 0.194 | −0.00481 |
| 5 | 0.163 | 0.00364 |
| 6 | 0.156 | 0.00627 |
| 7 | 0.137 | 0.000786 |
| 8 | 0.131 | −0.000435 |
| 9 | 0.118 | 0.00103 |
| 10 | 0.113 | 0.00163 |
| 11 | 0.103 | 0.000429 |
| 12 | 0.100 | 0.000196 |

Table 2. The critical thicknesses and values of $\lambda^2$ for several modes of an 8 × 6 cm plate subjected to a $T(x) = 1412 - 110.74x + 3.5x^2$ (°C). The initial dislocation density is 0.5 $cm^{-2}$ and the actual thickness $h$ used to calculate $\lambda^2$ was 1.1 $h_{cr}$ (0.217 mm) of the first mode. The fastest growing mode is the second one

| Mode | $h_{cr}$(mm) | $\lambda^2(s^{-1})$ |
|---|---|---|
| 1 | 0.198 | 0.00143 |
| 2 | 0.195 | 0.00238 |
| 3 | 0.154 | 0.0000212 |
| 4 | 0.148 | −0.000117 |
| 5 | 0.126 | 0.000135 |
| 6 | 0.119 | 0.000210 |
| 7 | 0.105 | 0.0000319 |
| 8 | 0.100 | −0.00000653 |
| 9 | 0.0904 | 0.0000443 |
| 10 | 0.0873 | 0.0000631 |
| 11 | 0.0796 | 0.0000240 |
| 12 | 0.0767 | 0.0000126 |

geometries) is twisting (see Fig. 5). The maximum lateral growing speed for an 8 cm wide ribbon is larger than that of a 6 cm wide ribbon which is in turn larger than that of a 4 cm wide ribbon with $h = 1.1\,h_{cr}$.

### 3.2. *The exponential thermal profile example*

Consider now the case of a plate of the same ribbon length (8 cm), same initial dislocation density (0.5 $cm^{-2}$) and same pull speed (3 cm $min^{-1}$) as used in the parabolic profile, but let the ribbon be subjected to the exponential thermal profile of the form $T(x) = 1440 \exp(-0.08x)$°C. The values of $\lambda^2$ are again calculated by assuming $h = 1.1h_{cr}$. The critical thicknesses and the values of $\lambda^2$ are contained in Tables 4–6 for ribbon widths of 7.5, 6 and 4 cm, respectively. Clearly, the second mode (bending) has the fastest lateral growing speed for the 7.5 cm wide ribbon. Results for a 6 cm wide ribbon are contained in Table 5. The second mode (bending + curling) has the maximum lateral growing speed. Table 6 contains results obtained for a 4 cm wide ribbon. However, in this case the buckling mode with the fastest lateral speed is the first one (twisting).

Table 3. The critical thicknesses and values of $\lambda^2$ for several modes of an 8 × 4 cm plate subjected to a $T(x) = 1412 - 110.74x + 3.5x^2$ (°C). The initial dislocation density is $0.5\,cm^{-2}$ and the actual thickness $h$ used to calculate $\lambda^2$ was $1.1\,h_{cr}$ (0.128 mm). The fastest growing mode is the first one

| Mode | $h_{cr}$ (mm) | $\lambda^2$ ($s^{-1}$) |
|---|---|---|
| 1 | 0.117 | 0.000353 |
| 2 | 0.108 | 0.000221 |
| 3 | 0.0914 | 0.00000618 |
| 4 | 0.0881 | −0.00000812 |
| 5 | 0.0775 | 0.0000275 |
| 6 | 0.0735 | 0.0000419 |
| 7 | 0.0651 | 0.00000934 |
| 8 | 0.0632 | −0.000000506 |
| 9 | 0.0572 | 0.0000115 |
| 10 | 0.0552 | 0.0000169 |
| 11 | 0.0506 | 0.00000701 |
| 12 | 0.0492 | 0.00000271 |

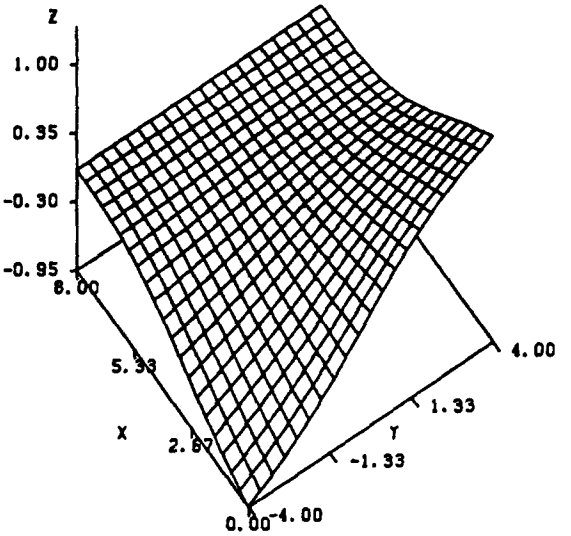


Fig. 5. The first buckling mode shape for an 8 × 8 cm plate subjected to the parabolic thermal profile $T(x) = 1412 - 110.74x + 3.5x^2$ (°C). The critical thickness is 0.262 mm. The initial dislocation density is $0.5\,cm^{-2}$.

## 4. DISCUSSIONS

The parameter used herein to describe the creep buckling resistance of plates is the thickness. This is a different parameter than is usually used in stability analyses of plates. The thickness is used here because $T(x)$ is fixed† and cannot be changed in magnitude and the in-plane thermal stresses in plates change with the width. The thermal stresses are obtained from the prebuckling state (plane stress problem), and then substituted into the buckling equation of plates to calculate the critical thickness and the corresponding buckling shape of plates.

It is found that in the case of thermal creep buckling of thin viscoplastic plates that the lowest mode does not always grow fastest. In fact it can damp out. By following Tvergaard's method[14] and using the Haasen–Sumino model, the thermal creep buckling equation can be derived in terms of the elastic lateral deflection $w^e$ and its rate $\dot{w}^e$. This

† In some industrial cases the thermal profile $T(x)$ may depend on the ribbon thickness. We do not consider this variation in our calculations.

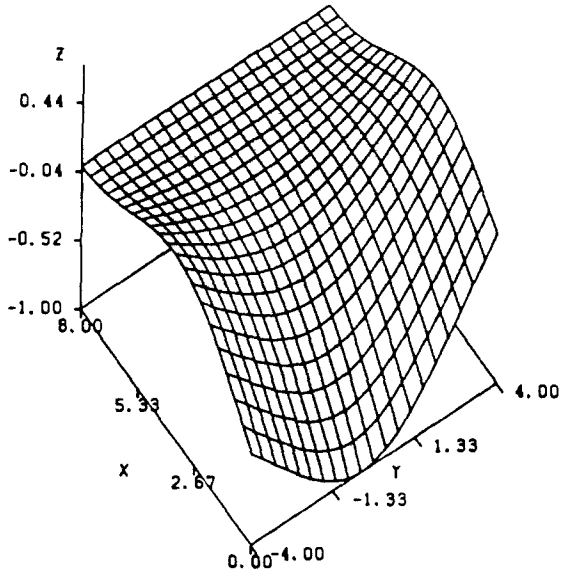


Fig. 6. The second buckling mode shape for the same case used in Fig. 5. The critical thickness is 0.258 mm.

Table 4. The critical thicknesses and values of $\lambda^2$ for several modes of an 8 × 7.5 cm plate subjected to a $T(x) = 1440\,e^{-0.08x}$ (°C). The initial dislocation density is 0.5 $cm^{-2}$ and the actual plate thickness $h$ used to calculate $\lambda^2$ was 1.1 $h_{cr}$ (0.254 mm). The fastest growing mode is the second one

| Mode | $h_{cr}$ (mm) | $\lambda^2$ ($s^{-1}$) |
|---|---|---|
| 1 | 0.231 | 0.0615 |
| 2 | 0.227 | 0.109 |
| 3 | 0.178 | −0.0000841 |
| 4 | 0.172 | −0.00621 |
| 5 | 0.144 | 0.00478 |
| 6 | 0.139 | 0.00777 |
| 7 | 0.121 | 0.00103 |
| 8 | 0.116 | −0.000398 |
| 9 | 0.104 | 0.00137 |
| 10 | 0.101 | 0.00209 |
| 11 | 0.0922 | 0.000556 |
| 12 | 0.0892 | 0.000323 |

equation is not limited to elastic plate buckling but rather applies to a plate simultaneously having both elastic and viscoplastic behavior. In this analysis, the value of $\lambda^2$ for silicon ribbon is dependent on the values of the viscosity $f$ and the critical thickness and the corresponding buckling mode shape. The critical thickness and corresponding mode shape are affected by the thermal profile and the in-plane dimensions of the ribbon. In this paper, several deflection shapes and values of $\lambda^2$ are reported. The lowest mode does not necessarily have the largest value of $\lambda^2$. The actual ribbon thickness has to be larger than the critical thickness of the lowest mode that is calculated from eqn (22), otherwise the value of $\lambda^2$ in eqn (17) becomes infinite and the plate will have a bifurcation type of buckling. Since the wider ribbon produces larger values of the in-plane stresses for the same thermal profile and also has a smaller resistance to buckling, wider ribbon generally has a greater critical thickness and a larger value of $\lambda^2$. Especially, when the width of the plate approaches the critical width mentioned above in value, a further small increment in width will result in a large change in the value of $\lambda^2$ and hence the speed of the lateral deflection. Since the ribbon thickness affects the speed of the lateral deflection, if a larger

Table 5. The critical thicknesses and values of $\lambda^2$ for several modes of an 8 × 6 cm plate subjected to a $T(x) = 1440e^{-0.08x}$ (°C). The initial dislocation density is 0.5 cm$^{-2}$ and the actual plate thickness $h$ used to calculate $\lambda^2$ was $1.1\,h_{cr}$ (0.216 mm). The fastest growing mode is the second one

| Mode | $h_{cr}$ (mm) | $\lambda^2$ (s$^{-1}$) |
|---|---|---|
| 1 | 0.196 | 0.00372 |
| 2 | 0.193 | 0.00599 |
| 3 | 0.152 | 0.0000110 |
| 4 | 0.146 | −0.000338 |
| 5 | 0.124 | 0.000316 |
| 6 | 0.118 | 0.000486 |
| 7 | 0.104 | 0.0000664 |
| 8 | 0.100 | −0.0000176 |
| 9 | 0.0894 | 0.0000995 |
| 10 | 0.0865 | 0.000141 |
| 11 | 0.0789 | 0.0000507 |
| 12 | 0.0761 | 0.0000263 |

Table 6. The critical thicknesses and values of $\lambda^2$ for several modes of an 8 × 4 cm plate subjected to a $T(x) = 1440\,e^{-0.08x}$ (°C). The initial dislocation density is 0.5 cm$^{-2}$ and the actual plate thickness $h$ used to calculate $\lambda^2$ was $1.1\,h_{cr}$ (0.131 mm). The fastest growing mode is the first one

| Mode | $h_{cr}$ (mm) | $\lambda^2$ (s$^{-1}$) |
|---|---|---|
| 1 | 0.119 | 0.000602 |
| 2 | 0.108 | 0.000364 |
| 3 | 0.0905 | 0.00000499 |
| 4 | 0.0876 | −0.0000254 |
| 5 | 0.0768 | 0.0000390 |
| 6 | 0.0730 | 0.0000697 |
| 7 | 0.0645 | 0.0000136 |
| 8 | 0.0628 | −0.00000634 |
| 9 | 0.0567 | 0.0000174 |
| 10 | 0.0549 | 0.0000273 |
| 11 | 0.0502 | 0.0000103 |
| 12 | 0.0489 | 0.00000291 |

thickness is used the speed will decrease. We found from calculations that the elastic critical thickness of ribbons is close to the viscoplastic critical thickness. For example, the critical thickness of the elastic ribbon is 0.251 mm while it is 0.231 mm for the viscoplastic ribbon in the case of an 8 × 7.5 cm ribbon subjected to the exponential thermal profile. Therefore, if we want to prevent all possibilities of elastic buckling and neglect the speed of the lateral deflection of creep buckling, the elastic buckling analysis can be used. A ribbon thickness which is larger than the calculated elastic critical thickness is suggested for use in the growth of silicon ribbon.

We note that reports in the silicon ribbon literature show many examples of long wavelength buckling mode shapes[4] of the type shown in Figs 5 and 6. We also note that examples of short wavelength buckling are also reported[2]. We interpret the latter as examples of cases where $\lambda^2 < 0$ for the lower modes but not for some of the higher ones. They occur in a more complex thermal profile than is used here.

## 5. CONCLUSIONS

(1) A governing equation of thermal viscoplastic buckling of plates based on the Haasen–Sumino material model was derived.

(2) The governing equation is separated into two differential equations. One equation is related to the lateral deflection shape of plates, and the other is related to the growing

speed of the lateral deflection of plates.

(3) The critical thicknesses and the corresponding lateral deflection shapes were calculated from the solutions of the governing equations. The lateral deflection speeds of thermal creep buckling were also computed. A positive speed indicates that the lateral deflection of the ribbon grows in time while a negative speed signifies that the lateral deflection of the ribbon decreases in value with time.

*Acknowledgements*—The writers would like to thank numerous colleagues in the JPL-DOE Solar Energy Flat Plate Project for their contributions to our program. Professor R. J. De Angelis has been extremely helpful throughout this entire project. We also thank Dr M. Leipold (JPL) for his initial help and Professor T. Gross (U.K.) and Tim O'donnell (JPL) for numerous conversations. Drs R. G. Seidensticker (Westinghouse), J. Spitznagel (Westinghouse), J. Kalejs (Mobil Solar) and R. Hartzell (Texas Instruments) have been of tremendous help with reports on the real world observations. This research was financed by JPL Contract No. 956571.

## REFERENCES

1. C. S. Duncan, R. G. Seidensticker, J. P. Mchugh and J. Schruben, Advanced dendritic web growth development, Annual Report, 23 October (1981)–22 October (1982), Westinghouse R and D Center, Pittsburgh, Pennsylvania.
2. J. P. Kalejs, B. H. Mackintosh and T. Surek, High speed EFG of wide silicon ribbon. *J. Crystal Growth* **50**, 175–192 (1980).
3. R. G. Seidensticker and R. H. Hopkins, Silicon ribbon growth by the dendritic web process. *J. Crystal Growth* **50**, 221–235 (1980).
4. R. G. Seidensticker and J. S. Schruben, Control of thermal stress in dendritic web growth. In *Proc. of the Flat-plate Solar Array Project Research Forum on the High-speed Growth and Characterization of Crystals for Solar Cells*, Port St. Lucie, Florida, July 1983, Jet Propulsion Laboratory Publication, 84-23. Pasadena, California (1984).
5. W. Gurtler, Nature of thermal stresses and potential for reduced thermal buckling of thin silicon ribbon grown at high speed. *J. Crystal Growth* **50**, 69–82 (1980).
6. O. W. Dillon, Jr. and R. De Angelis, On improved analysis of the thermal buckling of silicon sheet. In *Proc. of the Flat-plate Solar Array Project Research Forum on the High-speed Growth and Characterization of Crystals for Solar Cells*, Port St. Lucie, Florida, July 1983, Jet Propulsion Laboratory Publication, 84-23. Pasadena, California (1984).
7. P. Haasen, Zur Plastischen Verformuny Von Germanium und InSb. *Z. Phys.* **167**, 461–467 (1962).
8. P. Haasen, Dislocation dynamics in the diamond structure. In *Dislocation Dynamics* (Edited by A. R. Rosenfield, G. T. Hahn, A. L. Bemet, Jr. and I. Jaffee), p. 196. Battlelle Institute Materials Science Colloquia.
9. I. Yonengo and K. Sumino, Dislocation dynamics in the plastic deformation of silicon crystals, I. Experiments. *Phys. Stat. Sol.* (*a*) **50**, 685 (1978).
10. M. Suezava, K. Sumino and I. Yonenago, Dislocation dynamics in the plastic deformation of silicon crystals, II. Theoretical analysis of experimental results. *Phys. Stat. Sol.* (*a*) **51**, 217–226 (1979).
11. R. Gleichmann, B. Cunningham and D. G. Ast, Process-induced defects in solar cell silicon. *J. Appl. Phys.* **58**, 223–229 (1985).
12. K. Yang, G. H. Schwuttke and T. F. Ciszek, Structural and electrical characterization of crystallographic defects in silicon ribbon. *J. Crystal Growth* **50**, 301–310 (1980).
13. C. T. Tsai, Thermal visco-plastic stress and buckling analysis of silicon ribbon. Ph.D. Dissertation, Department of Engineering Mechanics, University of Kentucky, Lexington, Kentucky, December (1985).
14. V. Tvergaard, Creep buckling of rectangular plates under axial compression. *Int. J. Solids Structures* **15**, 441–456 (1979).
15. B. A. Boley and J. H. Weiner, *Theory of Thermal Stresses*. Wiley, New York (1965).
16. S. Timoshenko and Gere, *Theory of Elastic Stability*, 2nd Edn. McGraw-Hill, New York (1961).
17. R. Szilard, *Theory and Analysis of Plates—Classical and Numerical Methods*. Prentice-Hall, New York (1974).
18. R. Hartzell, Personal communication, Texas Instruments Corporation (1984).
19. O. W. Dillon, Jr., R. J. Deangelis and C. T. Tsai, Dislocation dynamics during the growth of silicon ribbon. Submitted for publication, February (1986).
20. A. Pifko and G. Isakson, A finite element method for the plastic buckling analysis of plates. *AIAA J.* **7**(10), 1950–1957 (1969).
21. F. K. Bogner, R. L. Fox and L. A. Schmit, The generation of interelement compatible stiffness and mass matrices by the use of interpolation formula. In *Proc. Conf. Matrix Methods in Struct. Mech.* Air Force Inst. of Tech., Wright Patterson A. F. Base, Ohio (1965).
22. K. T. Bathe and E. L. Wilson, *Numerical Methods in Finite Element Analysis*. Prentice-Hall, New York (1976).
23. O. G. Zienkiewicz, *The Finite Element Method*, 3rd Edn. McGraw-Hill, New York (1977).

## APPENDIX

Consider a simply supported rectangular plate with length $a$ and width $b$. For a simply supported plate, the deflections and the moments along the boundaries are zero, and the deflection shape can be assumed as

$$W(x, y) = \sin\left(\frac{i\pi x}{a}\right)\sin\left(\frac{j\pi y}{b}\right) \tag{A1}$$

where $i$ and $j$ are positive integers.

The values of the viscosity $f$ are calculated from the prebuckling state. The initial imperfection $w^0$ is also assumed to have the same shape as $W(x, y)$ of eqn (A1). That is

$$w^0 = g^0 W(x, y) \tag{A2}$$

where $g^0$ is the magnitude of the initial imperfection. The solution of eqn (15) can now be written as

$$w^e = g(t)\sin\left(\frac{i\pi x}{a}\right)\sin\left(\frac{j\pi y}{b}\right). \tag{A3}$$

By substitution of eqn (A3) into eqn (15), it becomes

$$\begin{aligned}\frac{D_e}{h}\dot{g}(t)\left[\left(\frac{i\pi}{a}\right)^4 + 2\left(\frac{i\pi}{a}\right)^2\left(\frac{j\pi}{b}\right)^2 + \left(\frac{j\pi}{b}\right)^4\right]\sin\left(\frac{i\pi x}{a}\right)\sin\left(\frac{j\pi y}{b}\right) = \\ -\left[\frac{2fE}{3}g(t) + \dot{g}(t)\right]\left[\sigma^0_{xx}\left(\frac{i\pi}{a}\right)^2\sin\left(\frac{i\pi x}{a}\right)\sin\left(\frac{j\pi y}{b}\right)\right. \\ \left. - 2\sigma^0_{xy}\left(\frac{i\pi}{a}\right)\left(\frac{j\pi}{b}\right)\cos\left(\frac{i\pi x}{a}\right)\cos\left(\frac{j\pi y}{b}\right) + \sigma^0_{yy}\left(\frac{j\pi}{b}\right)^2\sin\left(\frac{i\pi x}{a}\right)\sin\left(\frac{j\pi y}{b}\right)\right].\end{aligned} \tag{A4}$$

If the values of $E$, $\sigma^0_{xy}$, $\sigma^0_{xy}$ and dislocation density in the plate are assumed to be constant and $\sigma^0_{xy}$ to vanish, the values of $f$ are also constant and the term involving $\sigma^0_{xy}$ in eqn (A4) vanishes. Therefore, sin functions in both sides of eqn (A4) can be cancelled. Then, by rearranging the coefficients of $\dot{g}(t)$ and $g(t)$, and finally dividing both sides by the coefficient of $\dot{g}(t)$, we have

$$\dot{g}(t) - Bg(t) = 0. \tag{A5}$$

The value of $B$ is determined by the value of $f$, $E$, $\sigma^0_{yy}$ and $\sigma^0_{yy}$. That is

$$B = \frac{B1}{B2} \tag{A6}$$

where

$$\begin{aligned}B1 &= -\frac{2fE}{3}\left[\sigma^0_{xx}\left(\frac{i\pi}{a}\right)^2 + \sigma^0_{yy}\left(\frac{j\pi}{b}\right)^2\right] \\ B2 &= \frac{D_e}{h}\left[\left(\frac{i\pi}{a}\right)^4 + 2\left(\frac{i\pi}{a}\right)^2\left(\frac{j\pi}{b}\right)^2 + \left(\frac{j\pi}{b}\right)^4\right] \\ &\quad + \sigma^0_{xx}\left(\frac{i\pi}{a}\right)^2 + \sigma^0_{yy}\left(\frac{j\pi}{b}\right)^2\end{aligned}$$

and the solution of eqn (A5) becomes

$$g(t) = g^0(e^{Bt} - 1). \tag{A7}$$

From eqns (A6) and (A7), the value of the plate thickness $h$ and the in-plane forces control the speed of creep buckling. If the in-plane stresses $\sigma^0_{xx}$ and $\sigma^0_{yy}$ of eqn (A6) are tensile, the value of $B$ is negative and the initial imperfection $w^0$ of the plate will eventually damp out with time. On the other hand, if the in-plane forces are compressive, the lateral deflection of the plate grows with time. By substituting the prescribed deflection shape and the constant in-plane stresses $\sigma^0_{xx}$ and $\sigma^0_{yy}$ into the elastic buckling equation, the following equation is obtained:

$$\frac{D^{cr}_e}{h}\left[\left(\frac{i\pi}{a}\right)^4 + 2\left(\frac{i\pi}{a}\right)^2\left(\frac{j\pi}{b}\right)^2 + \left(\frac{j\pi}{b}\right)^4\right] + \sigma^0_{xx}\left(\frac{i\pi}{a}\right)^2 + \sigma^0_{yy}\left(\frac{j\pi}{b}\right)^2 = 0 \tag{A8}$$

where

$$D^{cr}_e = \frac{Eh^3_{cr}}{12(1-\nu^2)}.$$

From eqn (A8), the critical thickness $h_{cr}$ for the in-plane stresses $\sigma^0_{yy}$ and $\sigma^0_{yy}$ is

$$h^2_{cr} = -\frac{\sigma^0_{xx}\left(\frac{i\pi}{a}\right)^2 + \sigma^0_{yy}\left(\frac{j\pi}{b}\right)^2}{\left(\frac{i\pi}{a}\right)^4 + 2\left(\frac{i\pi}{a}\right)^2\left(\frac{j\pi}{b}\right)^2 + \left(\frac{j\pi}{b}\right)^4} \times \frac{12(1-\nu^2)}{E}. \tag{A9}$$

By substituting eqn (A9) into eqn (A6), we obtain

$$B = -\frac{\sigma^0_{xx}\left(\frac{i\pi}{a}\right)^2 + \sigma^0_{yy}\left(\frac{j\pi}{b}\right)^2}{\left(\frac{i\pi}{a}\right)^4 + 2\left(\frac{i\pi}{a}\right)^2\left(\frac{j\pi}{b}\right)^2 + \left(\frac{j\pi}{b}\right)^4} \times \frac{8f(1-\nu^2)}{(h^2 - h^2_{cr})} \tag{A10}$$

where $h > h_{cr}$ was implied during the derivation of eqn (A10). Therefore, when a plate is subjected to in-plane compressive forces, the value of $B$ is positive and the lateral deflection of the plate will grow with time according to eqn (A7). If $h$ is equal to $h_{cr}$, the value of $B$ becomes infinite and this means that bifurcation buckling occurs at "zero" time. This also reveals that a larger value of $h$ will cause the lateral deflection of the plates to grow more slowly. From the above behavior of creep buckling of plates for a simple case, the behavior for more complex problems can be better understood.

If the values of $f$, $E$, $\sigma^0_{xx}$, $\sigma^0_{xy}$ and $\sigma^0_{yy}$ are not constant and vary in space, Galerkin's method can be applied to eqn (A4) to calculate the value of $B$. That is, let

$$B = \frac{B3}{B4 + B5} \tag{A11}$$

where

$$B3 = \int_0^a \int_0^b \frac{2fE}{3}\left[\sigma^0_{xx}\left(\frac{i\pi}{a}\right)^2 \sin\left(\frac{i\pi x}{a}\right)\sin\left(\frac{i\pi y}{b}\right) - 2\sigma^0_{xy}\left(\frac{i\pi}{a}\right)\left(\frac{j\pi}{b}\right)\cos\left(\frac{i\pi x}{a}\right)\cos\left(\frac{j\pi y}{b}\right) + \sigma^0_{yy}\left(\frac{j\pi}{b}\right)^2 \sin\left(\frac{i\pi x}{a}\right)\sin\left(\frac{j\pi y}{b}\right)\right]\sin\left(\frac{i\pi x}{a}\right)\sin\left(\frac{j\pi y}{b}\right)dx\,dy$$

$$B4 = \left[\left(\frac{i\pi}{a}\right)^4 + 2\left(\frac{i\pi}{a}\right)^2\left(\frac{j\pi}{b}\right)^2 + \left(\frac{j\pi}{b}\right)^4\right]h^2 \times \int_0^a \int_0^b \frac{E}{12(1-\nu^2)}\sin^2\left(\frac{i\pi x}{a}\right)\sin^2\left(\frac{j\pi y}{b}\right)dx\,dy$$

and

$$B5 = \int_0^a \int_0^b \left[\sigma^0_{xx}\left(\frac{i\pi}{a}\right)^2 \sin\left(\frac{i\pi x}{a}\right)\sin\left(\frac{j\pi y}{b}\right) - 2\sigma^0_{xy}\left(\frac{i\pi}{a}\right)\left(\frac{j\pi}{b}\right)\cos\left(\frac{i\pi x}{a}\right)\cos\left(\frac{j\pi y}{b}\right) + \sigma^0_{yy}\left(\frac{j\pi}{b}\right)^2 \sin\left(\frac{i\pi x}{a}\right)\sin\left(\frac{j\pi y}{b}\right)\right]\sin\left(\frac{i\pi x}{a}\right)\sin\left(\frac{j\pi y}{b}\right)dx\,dy.$$